iScience

CellPress OPEN ACCESS

Article

An intermediate state in trans-differentiation with proliferation, metabolic, and epigenetic switching

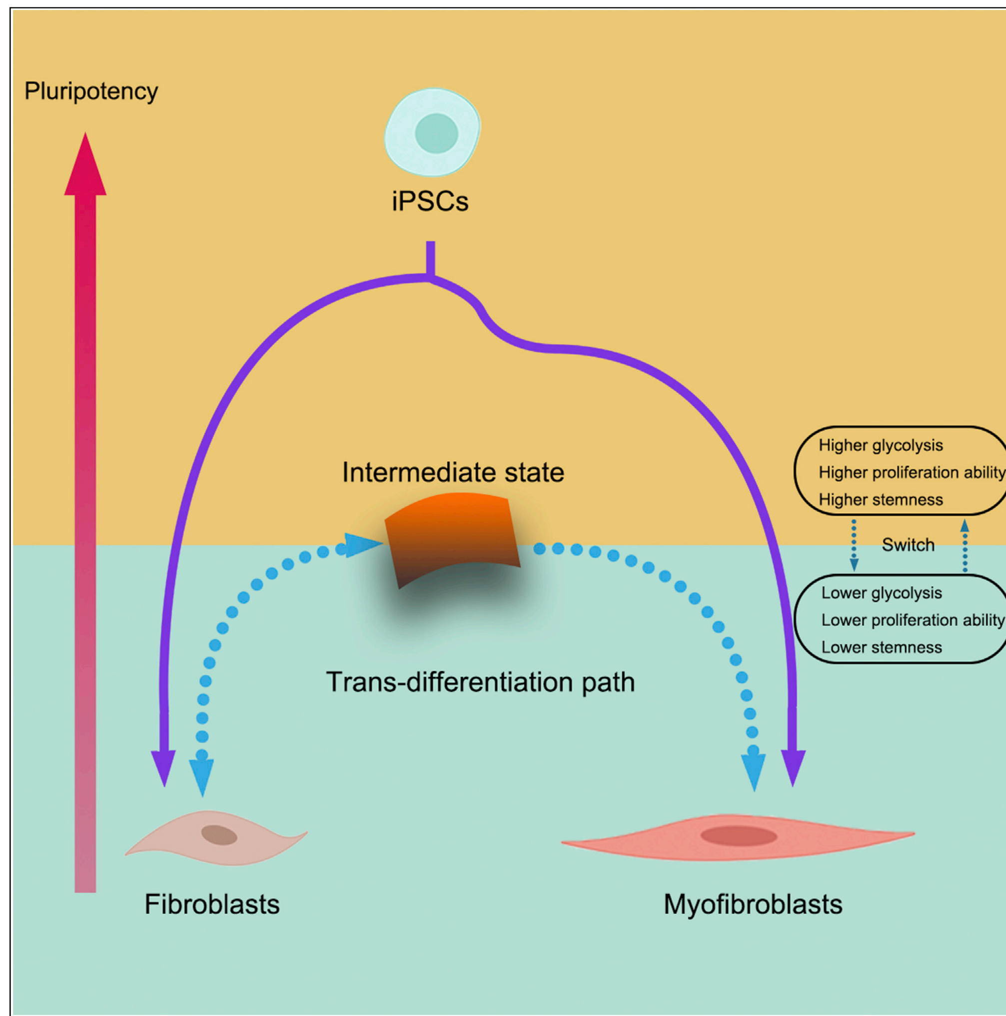

Zhikai Ye, Wenbo Li, Zhenlong Jiang, Erkang Wang, Jin Wang

jin.wang.1@stonybrook.edu (J.W.)
ekwang@ciac.ac.cn (E.W.)
jiangzl@ciac.ac.cn (Z.J.)

Highlights

Smads and Akt/p38MAPK pathways play the key role in fibroblast transition

There is a cell proliferation capability switching induced by TGF-β1

Metabolic reprogramming is required during trans-differentiation

An intermediate state appeared with high pluripotency in trans-differentiation

Ye et al., iScience 24, 103057
September 24, 2021 © 2021 The Author(s).
https://doi.org/10.1016/j.isci.2021.103057

CellPress
OPEN ACCESS

Article

An intermediate state in trans-differentiation with proliferation, metabolic, and epigenetic switching

Zhikai Ye,[1,2] Wenbo Li,[1] Zhenlong Jiang,[1,*] Erkang Wang,[1,2,*] and Jin Wang[3,4,*]

SUMMARY

Although TGF-β signaling can effectively activate fibroblasts to transform to myofibroblasts, the underlying mechanisms involved in the cell fate switching for trans-differentiation have not been fully elucidated. In this study, we found the evidence of an intermediate state in the process of trans-differentiation. In the early stage of trans-differentiation, cells enter the intermediate state first with multiple characteristics such as accelerating cell cycle, metabolic switching, enhanced anti-apoptotic ability, and pluripotency, which is very similar to the early stage of reprogramming. As the trans-differentiation continues, these characteristics get switched. Therefore, trans-differentiation appears to require the switching of cell proliferation ability, metabolic pathway, and "stemness" to complete the process. In this study, we can conclude that an intermediate state may be necessary with high pluripotency in trans-differentiation from fibroblasts to myofibroblasts. Only after passing the intermediate state, the trans-differentiation is finally completed and will not easily return to the original state.

INTRODUCTION

In response to various indicators of stress or damage, including physical stress, inflammatory mediators, growth factors, and cytokines, fibroblasts may become activated, eventually undergoing a phenotype switching to myofibroblasts (Roche et al., 2015), which is a typical trans-differentiation process. The TGF-β (transforming growth factor β)/Smad signaling pathway has long been known to be involved in this process and is arguably one of the most potent inductive mechanisms: TGF-β drives fibroblasts activation via the activation of phosphorylation of Smad2 and Smad3, which are complexed with Smad4, translocate to the nucleus, and form a transcriptional complex which can recruit the transcriptional co-activators to induce transcription of target genes including α-smooth muscle actin (α-Sma) and ECM (extracellular matrix) genes such as those encoding type I collagen (Roche et al., 2015; Ten Dijke et al., 2002). TGF-β may also work via a parallel non-canonical signaling pathway involving the activation of MAPK (mitogen-activated protein kinase) signaling to promote the expression of α-Sma (Zeglinski et al., 2016).

Although these results were used to explain the formation of myofibroblasts, the comprehensive mechanisms governing fibroblasts to myofibroblasts trans-differentiation are not yet fully elucidated. In mesenchymal cells (such as fibroblasts), TGF-β can stimulate or inhibit the cell proliferation by low and high concentrations of TGF-β, respectively (Liu et al., 2008). The role of this bidirectional effect has not been clearly clarified in the trans-differentiation process of fibroblasts. Another issue is that the transition of metabolic pathway from phosphorylation to glycolysis is thought to facilitate the differentiation of myofibroblasts (Lai et al., 2019; Sun et al., 2020). However, an experimental result showed the opposite effect that the glycolytic pathway did not affect the switching process (Schruf et al., 2019). Whether the "stemness" of the fibroblasts has changed during the trans-differentiation process was also ambiguous (Jopling et al., 2011). Another important question is whether the cells go through specific path and whether there exists a "stemness" intermediate state during the trans-differentiation process. This is crucial for its potential application in regenerative medicine and disease modeling (Granados-Aparici et al., 2019; Lu et al., 2013; Reid and Tursun, 2018; Ten Dijke et al., 2002; Wang et al., 2011).

In order to further explore the specific pathways and mechanisms involved in the trans-differentiation of fibroblasts into myofibroblasts, TGF-β induction was performed for different periods in this study. Then,

[1]State Key Laboratory of Electroanalytical Chemistry, Changchun Institute of Applied Chemistry, Chinese Academy of Sciences, Changchun, Jilin 130022, China

[2]University of Science and Technology of China, Hefei, Anhui 230029, P. R. China

[3]Department of Chemistry, Physics and Applied Mathematics, State University of New York at Stony Brook., Stony Brook, NY 11794-3400, USA

[4]Lead contact

*Correspondence: jin.wang.1@stonybrook.edu (J.W.), ekwang@ciac.ac.cn (E.W.), jiangzl@ciac.ac.cn (Z.J.)

https://doi.org/10.1016/j.isci.2021.103057

© 2021 The Author(s).
This is an open access article under the CC BY-NC-ND license (http://creativecommons.org/licenses/by-nc-nd/4.0/).

the time course analysis of the transcriptome expressions, proliferation capacity, and the metabolic reprogramming was adopted. The expression of a large number of genes in cell cycle pathways and metabolic pathways showed a non-monotonic trend in the trans-differentiation process. Correspondingly, we have also seen the switching of cell proliferation ability and metabolic pathways in the cell experiments. Furthermore, epigenetic factors including Ctcf, Ezh2, Kdm2b, and Wdr5 showed an upregulated and downregulated expression trend, which also suggested a switch in cell "stemness". These results provide the evidences of an intermediate state with high pluripotency in the early stage of trans-differentiation, which was associated with the metabolic OGS (switch from oxidative phosphorylation to glycolysis) and enhanced proliferation capability. Knockdown of Smad and Akt/p38MAPK signaling pathways will abrogate TGF-β-mediated trans-differentiation. All the data sculpted the whole trans-differentiation scenario from fibroblasts into myofibroblasts with an intermediate state, beyond which the cells will be difficult to come back. We believe that the evidence of the intermediate state and the formation mechanisms are important for understanding the trans-differentiation process between other lineages.

RESULTS

Sequential induction of trans-differentiation process

TGF-β pathway can effectively induce the transformation of skin cells into muscle fibroblasts. We induced HDFs (human dermal fibroblasts) (mesenchymal cells) with 5 ng/mL TGF-β1 for 1–7 days, respectively, and detected the marker gene α-Sma of muscle fibroblasts. In Figure 1A, we can see that the expression of marker gene α-Sma gradually increased with induction, and the expression level of α-Sma gradually reached the plateau after the fifth day, indicating that the trans-differentiation process was nearly completed. The further qPCR (quantitative real-time PCR) analysis of the expression of α-Sma, Fibronectin, and Col1a1 from day 7 to day 9 showed no significantly difference (Figure S1A). It also suggested that the trans-differentiation process was basically completed after the fifth day. It is generally believed that the downstream of TGF-β mainly includes the Smad pathway and the non-canonical PI3K/Akt pathway and MAPK pathway (Xie et al., 2015; Zhang et al., 2019). Therefore, we explored whether the Smad pathway and the Akt/p38MAPK pathway are indispensable in the trans-differentiation. siRNA of Smad4 and of Map2k6 were added before starvation (day -1), respectively. When Smad4 or Map2k6 was knocked down by siRNA, the expression of α-Sma at day 4 or day 7 was decreased. When knocking down both of them, the expressions of α-Sma would be significantly suppressed (Figure 1B). That is to say, siRNA-mediated knockdown of Smad and Akt/p38MAPK signaling pathways significantly attenuate the expression of α-Sma.

To further clarify whether the knockdown of Smad4 or Map2k6 just delays the trans-differentiation or abrogates the trans-differentiation and to exclude the possible effect of siRNA degradation, the siRNA was added during the trans-differentiation at day -1, day 2, and day 5. Although the expressions of several marker genes (α-Sma, Fibronectin, and Col1a1) would still be enhanced with the increase of the induction time after the addition of single type of siRNA (siRNA-Smad4 or siRNA-Map2k6), there were little changes in these genes by knocking down both of the Smad4 and the Map2k6 continuously. This indicates that the trans-differentiation was effectively blocked (Figure S1B). Meanwhile, the immunofluorescence staining of α-Sma, Fibronectin, and Col1a1 also showed that knocking down both of Smad4 and Map2k6 can effectively inhibit the trans-differentiation process (Figures 1C and S1C). In other words, the Smad pathway and the Akt/p38MAPK pathway can promote the trans-differentiation, respectively, and only knocking down one of them cannot completely prevent trans-differentiation. This illustrates that both the Smad pathway and the Akt/p38MAPK pathway together play the essential role in the trans-differentiation process.

Time course RNA sequencing of trans-differentiation

Although we can observe that the Smad pathway and the Akt/p38MAPK pathway play a key role in the process of trans-differentiation, the full process of trans-differentiation is still elusive. Trans-differentiation as a way of cell fate switching is a complex process, there must be a large number of cross-talk signaling pathways involved. In order to clarify the specific mechanism of trans-differentiation and gain a deep understanding from global perspective at the gene level, time course RNA sequencing is required. For the expressions of the marker genes, our time course RNA sequencing lasted until the seventh day. Then, the mRNA levels of the marker genes (Fibronectin and Col1a1) and the downstream genes of TGF-β signaling pathway (Snail1, Cdh2, and Zeb1) from day 5 to day 7 showed no obvious difference, which further suggested that the trans-differentiation process at day 7 was completed (Figure S2). Then, the expressions

CellPress
OPEN ACCESS

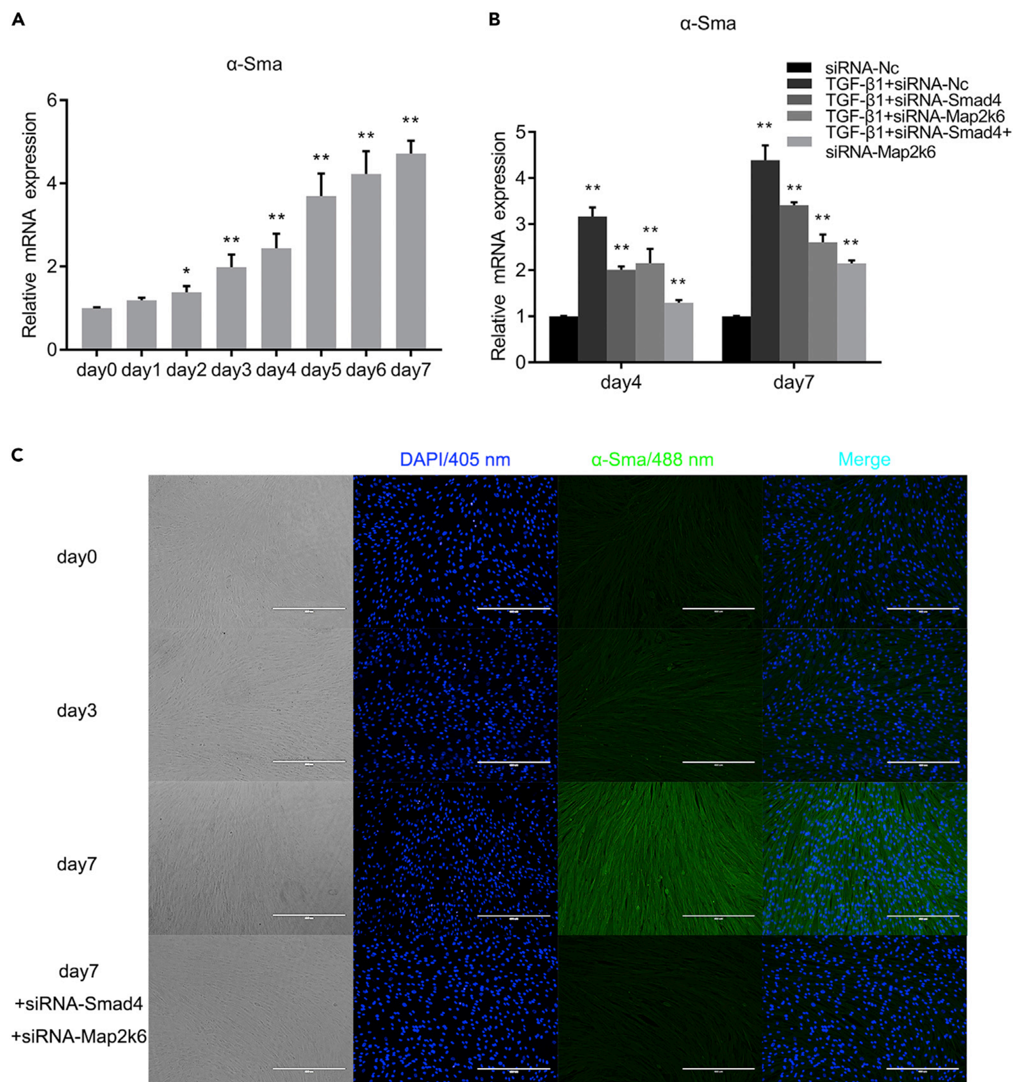

Figure 1. Knockdown of Smad and Akt/p38MAPK pathways inhibits trans-differentiation

(A) qPCR analysis of the expression of α-Sma after TGF-β1 continuously induced HDFs from day 0 to day 7. Data were presented as mean ± SD, n = 3. 0.01 < *P < 0.05, **P < 0.01 versus day0.

(B) qPCR analysis of the expression of α-Sma was measured at day 4 and day 7. HDFs induced by TGF-β1 after knockdown of Smad4, Map2k6, and both of them by siRNA before starvation, respectively. Data were presented as mean ± SD, n = 3. **P < 0.01 versus siRNA-Nc.

(C) Immunofluorescence staining during the trans-differentiation of α-Sma at day 0, day 3, and day 7 and knockdown of Smad4 and Map2k6 (bar, 400 μm). The siRNA of Smad4 and Map2k6 was added at day -1, day 2, and day 5, respectively.

of important differential genes from day 0 to day 7 were demonstrated by the heatmap (Figure 2). Although the change trend of most differential genes was the same as expected being relatively monotonic, some genes still showed surprising changes. After comparing the expression of differential genes in the whole trans-differentiation process, there were some interesting behaviors appeared in the cell cycle and metabolic pathway, which can also be affected by TGF-β. We can see that a large number of genes involved in the regulation of cell cycle and glycolysis in these two pathways show a completely different expressions trend in the early and late stages of trans-differentiation. For example, the expression of Akt1, Ras, Ldha, Hk, and a large number of CDK genes showed a trend of upregulation and then downregulation during the time sequence induction process. These genes are known to play an important role in promoting cell cycle and glycolytic metabolism. On the other hand, the genes that inhibit cell proliferation, such as Tp53, P16, and P21, showed an opposite expression trend, which was downregulated first and then

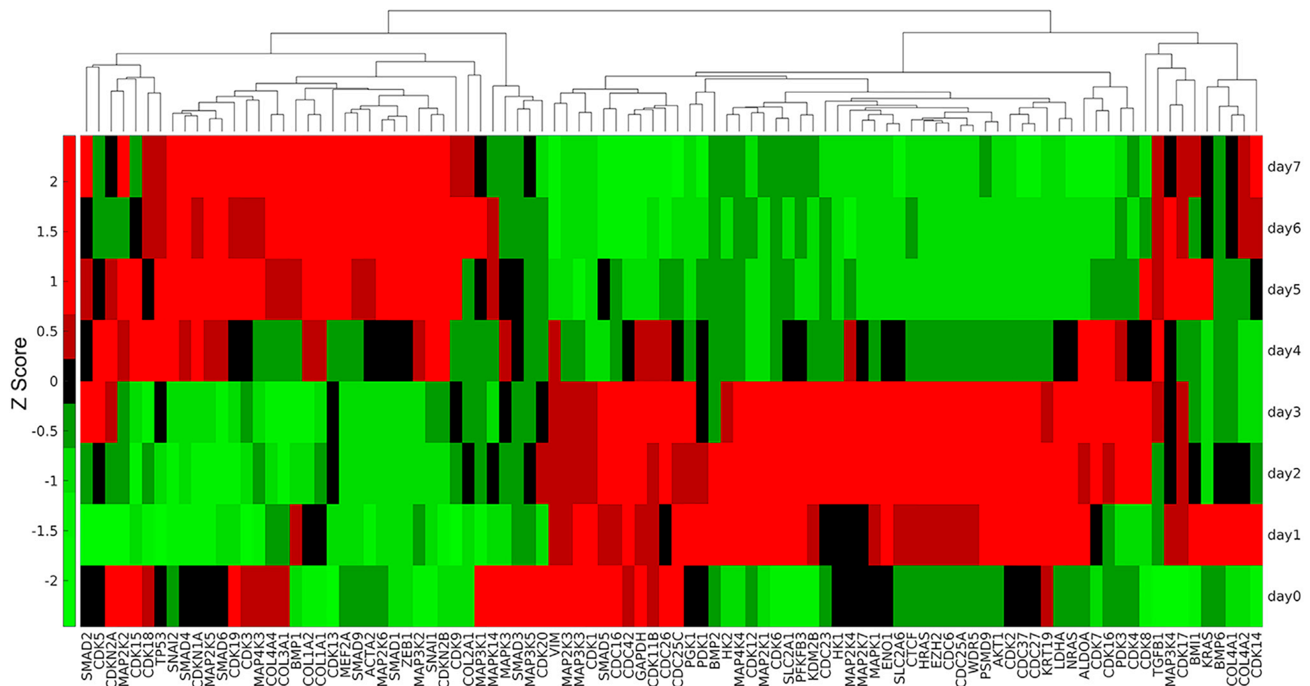

Figure 2. Time course RNA sequencing analysis and the heatmap of related genes during trans-differentiation

The global profile of gene expression was measured by time course RNA sequencing during trans-differentiation from day 0 to day 7. The red represents values above the mean, while black represents the mean and green represents values below the mean. Three independently repeated samples were collected for each test.

upregulated. Therefore, by analyzing the time course transcriptomic data, we can find that there was a state with the cell proliferation ability enhanced, glycolytic metabolism increased, and epigenetic barriers for pluripotency reduced in the initial stage of trans-differentiation, which would then return to the normal levels later. This behavior demonstrated a distinct particular turning point at day 3 or day 4. It showed that there was a distinct state in the early stage of trans-differentiation, similar to the state of cells in the early stage of reprogramming (Sun et al., 2020). On the other hand, some recent studies have suggested that epithelial cells may have an intermediate state in the process of EMT (Jolly et al., 2015; Yang et al., 2020). Here, we suppose that the cells may go through a clear intermediate state in the process of trans-differentiation from fibroblasts to myofibroblasts, and the trans-differentiation would be completed after passing through the intermediate state.

Switching of cell proliferation during trans-differentiation

In order to further confirm the reliability of the time course RNA sequencing results, we tested the growth rates of the cells at different time points during trans-differentiation. As can be seen from Figure 3A, the proliferation ability of the cells was gradually enhanced in the first 3 days after induction. However, the proliferation ability of the cells decreased significantly with induction from day 4. Although the switching of proliferation ability kept consistent with the results of RNA sequencing, the origin of this behavior still needs to be explored. As previously reported, the Smad pathway may inhibit the cell cycle (Granados-Aparici et al., 2019; Ten Dijke et al., 2002; Yeh et al., 2019). Therefore, we suggest that with the prolongation of trans-differentiation induction time, the decrease of the cell proliferation ability may be related to the activation of Smad pathway. In order to verify our hypothesis and to further confirm the influence of the Smad pathway on the cell proliferation in the process of trans-differentiation, we introduced SIS3, a small molecule which can effectively inhibit the Smad pathway. According to the qPCR results in Figure 3B, we can see that adding SIS3 can effectively improve the expression level of Akt1. At the same time, we also tested the cell proliferation ability. From Figure S3, it can be seen that the proliferation ability of the cells in the experimental group with SIS3 is significantly improved at 1 μM. Therefore, we inferred that the reason why cell proliferation first increased and then decreased in the induction process is closely related to the activation of Smad pathway. TGF-β activated the Akt/p38MAPK pathway during the initial induction period

CellPress
OPEN ACCESS

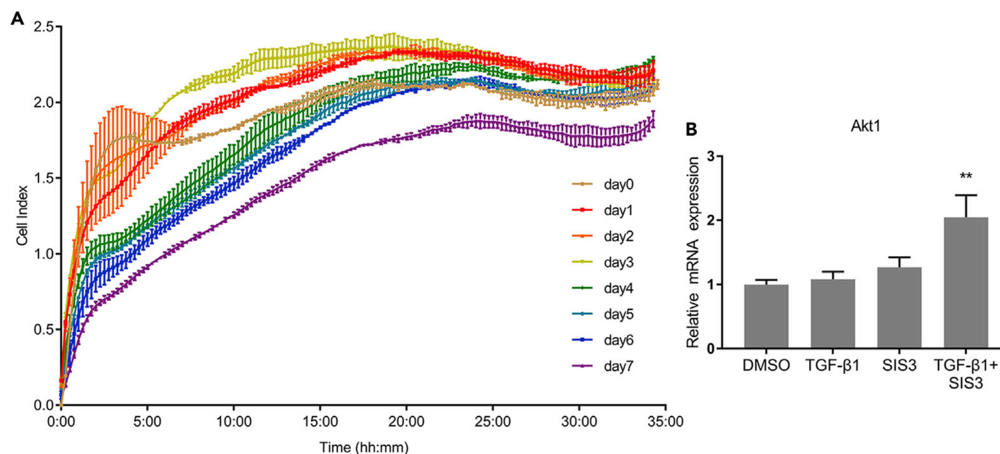

Figure 3. Changes in cell proliferation during trans-differentiation

(A) The cell index during cell proliferation from day 1 to day 7, respectively. The cell index was observed every 15 min for 30 hr for each group after TGF-β1-mediated fibrosis was finalized, and the cells were reseeded into E-plates.

(B) The mRNA levels of Akt1 at day 3 after treating with DMSO (blank), TGF-β1 (5 ng/mL), SIS3 (1 μM), and both of them, respectively. Data were presented as mean ± SD, n = 3. **P < 0.01 versus DMSO-treated group.

(0-3 days), which accelerated the cell cycle. At this time, the Smad pathway has not been activated effectively. With the induction progresses (4-7 days), the expressions of major components such as Smad2 and Smad4 were continuously enhanced (Figure 2), the Smad pathway was fully then activated, and cell proliferation was gradually inhibited.

Metabolic reprogramming from fibroblasts to myofibroblasts

The switching of the cell fate is often accompanied by metabolic reprogramming (Hua et al., 2020; Lai et al., 2019; Li et al., 2020). Furthermore, the cell proliferation requires metabolic pathways to provide energy, so changes in the cell proliferation capacity also require changes in metabolic pathways (DeBerardinis et al., 2008; Fritz and Fajas, 2010; Jones et al., 2005). Therefore, in order to better understand the process of trans-differentiation from fibroblasts to myofibroblasts, we need to test the changes in metabolic pathways. First of all, we analyzed the expressions of core genes in the metabolic pathway and found that Ldha, Hk1, Hk2, Pfk2, Glut1, Eno1, and other genes promoting OGS (switch from oxidative phosphorylation to glycolysis) showed an initial upregulated and then downregulated expression trend, which corresponded to the trend of cell proliferation ability during trans-differentiation. To further elucidate the role of metabolic pathways in trans-differentiation, glycolytic function (represented by extracellular acidification rate; ECAR) and mitochondrial respiration (represented by oxygen consumption rate; OCR) were determined by Seahorse analysis from day 0 to day 7 (Figures 4A and 4C). With ECAR tested, the glycolysis (induced by glucose) and glycolytic capability (induced by oligomycin) augmented from day 0 to day 3 then decreased from day 3 to day 7 (Figure 4B). For OCR, the basal respiration and ATP production (induced by FCCP) decreased from day 0 to day 4 and then augmented from day 4 to day 7 (Figure 4D). We can see that the change of glycolysis capacity and the change of cell proliferation capacity during trans-differentiation process form a clear correspondence. This indicates that there is across talk between these two pathways. Therefore, we have the reason to guess that the first increase and then decrease of glycolytic capacity is also related to the activation of the Smad pathway (Liang et al., 2020).

To verify this hypothesis, we tested the effect of TGF-β1 and SIS3 on glycolysis capacity. According to Figures S4A and S4B, we can see that the addition of TGF-β1 and SIS3 can promote the glycolysis ability of the cells. When TGF-β1 and SIS3 were added at the same time, the expressions of genes involved in glycolysis and glycolysis capacity were significantly enhanced (Figure S4C). Therefore, we proposed that due to the cross talk between glycolytic metabolism pathway and cell proliferation pathway, the effect of TGF-β pathway on the two is similar. In the initial stage of induction (0-3 days), Smad pathway was not effectively activated, while other pathways downstream of TGF-β such as Akt/p38MAPK pathway can effectively activate the glycolytic pathway. However, with the extension of induction time and the effective activation of Smad pathway, the glycolysis process was gradually inhibited, and the oxidative phosphorylation process

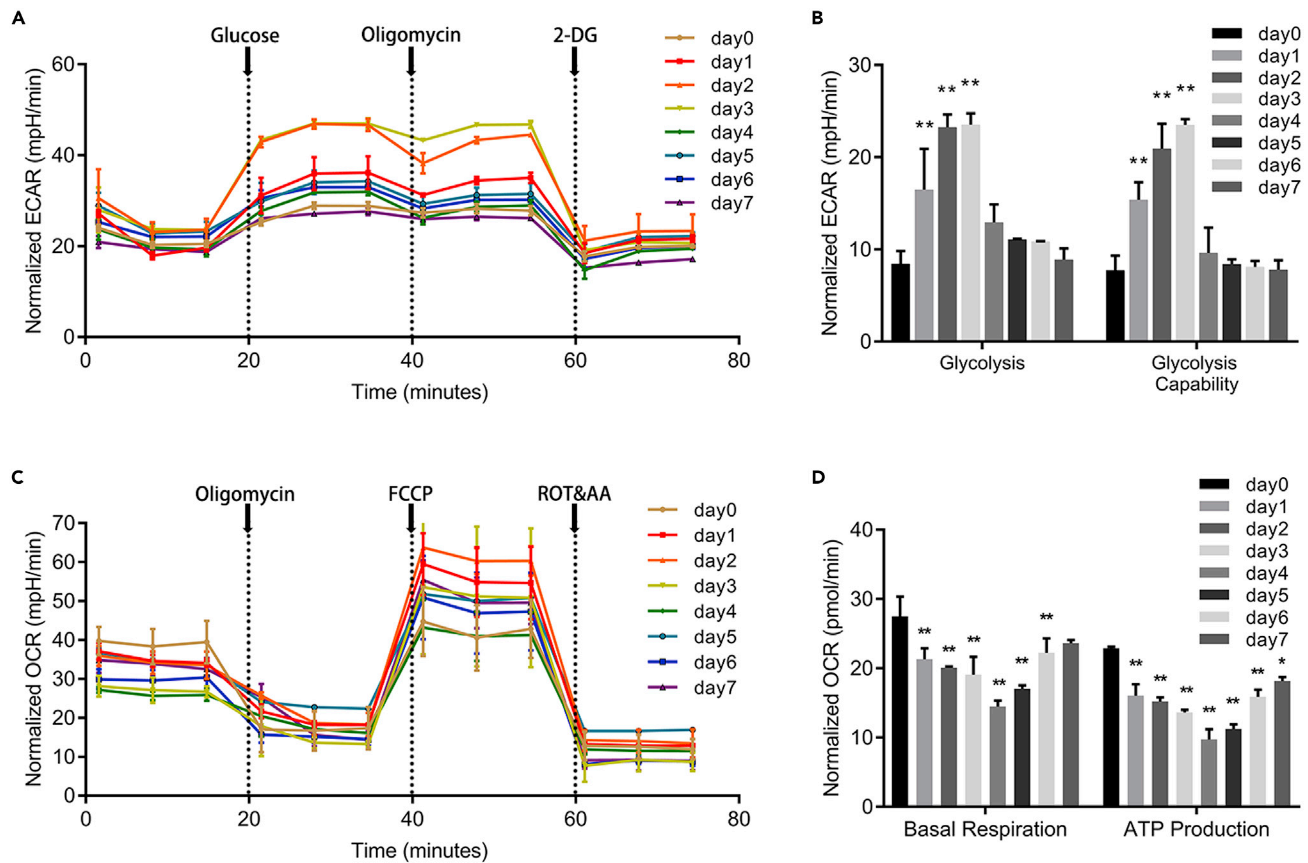

Figure 4. Metabolic switch during trans-differentiation

(A) and (B) Glycolysis function from day 0 to day 7 during trans-differentiation determined by Seahorse.

(B) Switch of glycolysis and glycolysis capability.

(C) and (D) Mitochondrial respiration from day 0 to day 7 during trans-differentiation determined by Seahorse.

(D) Alterations in basal respiration and ATP production. Data were presented as mean ± SD, n = 3. 0.01 < *P < 0.05, **P < 0.01 versus day0.

was gradually strengthened. That is to say, metabolic reprogramming is involved in the whole trans-differentiation process.

At the intermediate state, cells exhibit high pluripotency

Through the analysis of cell proliferation and metabolic switching in the process of trans-differentiation, we could find that there is a stage of enhanced cell proliferation and OGS in the initial stage of trans-differentiation process, and this feature was very similar to the initial stage of the reprogramming. Therefore, to further explore the association between the trans-differentiation and the reprogramming, we analyzed the expressions of the genes and epigenetic factors associated with the "stemness". We found that the expressions of Ctcf, Ezh2, Kdm2b, and Wdr5, four epigenetic factors, were significantly upregulated at the initial stage of induction and gradually downregulated in the subsequent induction process (Figure 5A). The increased expressions of the four epigenetic factors were reported to be effective in reducing barrier of pluripotency (Ang et al., 2011; Onder et al., 2012; Wang et al., 2011, 2017). Correspondingly, the expression of Tp53 gene which regulated apoptosis was downregulated at the early stage of trans-differentiation. In other words, in the switching process from fibroblasts to myofibroblasts, there is a state of accelerated cell cycle, improved glycolysis ability, enhanced anti-apoptosis ability, and reduced pluripotency barrier. That is to say, there is evidence of an intermediate state in the trans-differentiation process, which exhibits characteristics similar to those of early reprogramming. Further with the induction, the characteristics of pluripotency gradually disappeared. After the switching of "stemness", the fibroblasts gradually passed through the intermediate state, and the trans-differentiation was nearly completed.

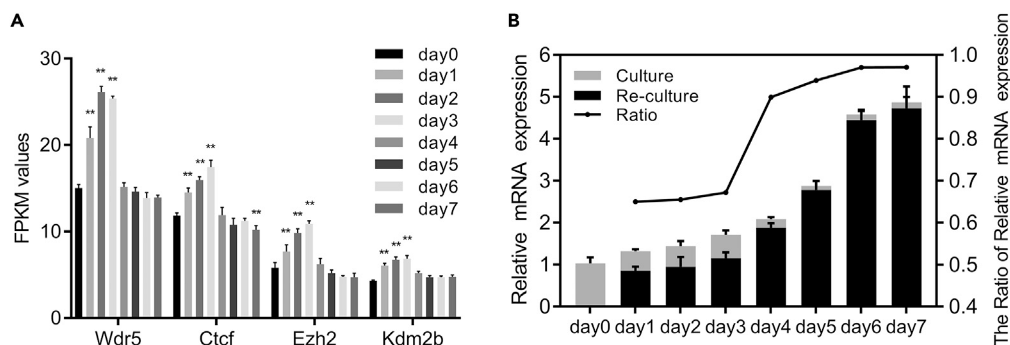

Figure 5. The intermediate state exhibited high pluripotency

(A) The FPKM values of four epigenetic factors (Ctcf, Ezh2, Kdm2b, and Wdr5) determined by RNA sequencing from day 0 to day 7. Data were presented as mean ± SD, n = 3. **P < 0.01 versus day0.

(B) Comparison of the expression of α-Sma by qPCR analysis between the cells in trans-differentiation and re-culturing for extend 3 days without treatment of TGF-β1. The gray columns represent the expression of α-Sma with sequential induction. The black columns represent the expression of α-Sma after TGF-β1 removal and re-culture for 3 days. The black line represents the ratio of these two sets.

In order to further verify whether this state is truly an intermediate state on the path of trans-differentiation, we reseeded the cells that have been induced for 1-7 days into the medium without TGF-β1 and continued to re-culture for 3 days. Further, we performed qPCR for the α-Sma expressions of the cells before and after re-culture. From Figure 5B, we can see that with the extension of the induction time, the expression of α-Sma in the cells after re-culture and the original culture was getting closer and closer. Especially from the fourth day, after 3 days of re-culture in the medium without TGF-β1, the expressions of α-Sma in the cells were almost undiminished, indicating that the cells have passed through the intermediate state and the cell fate has completed the switching from fibroblasts to myofibroblasts. It is suggested that the process of trans-differentiation must go through an intermediate stage similar to the early pluripotency state with multiple "stemness" traits. With the removal of TGF-β1, cells that stayed at the intermediate state will go back to fibroblasts, but it does not affect the trans-differentiation once the cells pass through the intermediate state.

DISCUSSION

Trans-differentiation from fibroblasts to myofibroblasts attracts attentions because of the important implications in wound healing, organ fibrosis, and regenerative medicine (Li and Wang, 2011; Smith, 2018; Tomasek et al., 2002). Although studies have demonstrated that TGF-β/Smad pathway is indispensible *in vitro* and *in vivo* for the process of fibroblasts trans-differentiation, the concrete mechanism is still unclear (Conte et al., 2014; Rodriguez et al., 2019). In this study, we investigated the TGF-β1-induced trans-differentiation to clarify the possible mechanism. As known, the Smad pathway activates the expression of α-Sma and promotes fibroblasts trans-differentiation (Meng et al., 2016). However, the role of the Akt/p38MAPK pathway in the trans-differentiation has not been clearly elucidated. To further investigate the role of the Smad and the Akt/MAPK pathway in the trans-differentiation by siRNA, we found that the trans-differentiation is closely related to the TGF-β/Smad and the Akt/p38MAPK signaling pathways, without which the trans-differentiation would not be continued (Figures 1B and S1B). When the siRNA of Smad4 and Map2k6 was added, respectively, we found that although the expression of α-Sma was suppressed to some extent, it would increase with the extension of induction time. This indicates that trans-differentiation still continued. Only by knocking down both of the Smad4 and Map2k6 simultaneously, the trans-differentiation would be abrogated. This illustrates that both the Smad pathway and the Akt/p38MAPK pathway together play an essential role in the trans-differentiation process.

To further clarify the role of the TGF-β/Smad and Akt/p38MAPK pathways in trans-differentiation, the time course RNA sequencing was performed to provide a global analysis of differential gene expressions. We performed the experiments and the associated time course analysis of the transcriptome expressions for 0-7 days. We found that the gene expressions exhibit a distinct dividing line at day 3 or day 4 during the time sequence induction process (Figure 2). After day 3 or day 4, the expression of some genes related

to Smad pathways exhibited a significant improvement, while the expression trends of many genes related to Akt/p38MAPK pathway were reversed. This suggests that there may be an intermediate state in the process of trans-differentiation at day 3 or day 4. As known, Akt/p38MAPK signaling can promote cell proliferation and glycolysis ability (Bolanos, 2013; Chang and Karin, 2001). So, we further analyzed the changes in the cell proliferation capacity and metabolic reprogramming in the process of trans-differentiation to confirm the results of RNA sequencing. During the initial induction period (0-3 days), the proliferation and aerobic glycolysis ability were continuously increased. With the further extension of the induction time (4-7 days), cell proliferation and aerobic glycolysis ability showed opposite trends (Figures 3A and 4). These results further suggest the existence of intermediate states during the trans-differentiation.

Therefore, we observed an interesting process that the glycolysis ability increased first and then decreased in this study. For the increase in the glycolysis ability during the trans-differentiation from fibroblasts to myofibroblasts, some previous work also confirmed the results. For example, during treatment with TGF-β1, the rapid augmentation of glycolysis accompanied with the slow change of mitochondrial respiration indicates that lung fibroblasts exhibit the features of aerobic glycolysis (Xie et al., 2015). Additionally, OGS is necessary for renal fibrosis which was restrained by the inhibition of aerobic glycolysis (Ding et al., 2017). Since glycolysis is essential in the process of trans-differentiation, a natural question to ask is why the glycolysis is gradually inhibited in the later stages of trans-differentiation. It has been reported that cell proliferation and metabolism is regulated by TGF-β/Smad signaling pathway which exhibits opposite effect to Akt/p38MAPK signaling pathway in many cell types (Ten Dijke et al., 2002). Smad4 activates P21 to inhibit cell proliferation and aerobic glycolysis ability (Hinz and Jucker, 2019; Pardali et al., 2005). Combined with the results of RNA sequencing (Figure 2), we reason that the Smad pathway inhibits the function of the Akt/p38MAPK pathway progressively, which results the inhibition of the glycolysis and cell proliferation. TGF-β rapidly activates the Akt/p38MAPK pathway during the early stage (0-3 days), which promotes the cell cycle and OGS. At this time, the Smad pathway has not been activated effectively. As the induction progresses (4-7 days), the expressions of the major components such as Smad2 and Smad4 are continuously enhanced; the Smad pathway is then fully activated. Consequentially, the cell proliferation and aerobic glycolysis ability are gradually inhibited. Then, the trans-differentiation process is completed. To further verify our hypothesis, we used SIS3 to inhibit the effect of the Smad pathway. From Figures S3 and S4, we could see that after the introduction of SIS3, the glycolysis ability and proliferation ability of cells have been significantly improved. This result further supports our inference. This may also give a possible explanation for bidirectional effect of TGF-β in cell proliferation and why do some experiments suggest that glycolysis does not play a key role in lung fibroblasts trans-differentiation, at least partially (Liu et al., 2008; Schruf et al., 2019). And we can see that, the metabolic switching involved in the whole induction process significantly promotes the fibroblast trans-differentiation.

Here, we also notice other interesting behaviors. At the early stage of trans-differentiation (0-3 days), compared with the significant increase in glycolysis, the changes in OXPHOS (oxidative phosphorylation) are moderate. In another work, Xie et al. showed a similar result that glycolysis activity is enhanced during the trans-differentiation from lung fibroblasts to myofibroblasts under the treatment by TGF-β1 in 24 hr, while OXPHOS mostly retained its activity (Xie et al., 2015). This suggests that fibroblasts may acquire a hybrid metabolic state where both glycolysis and OXPHOS are actively used. The hybrid metabolic phenotype has also been observed in immune cells and cancer cells, which may increase the metabolic plasticity and proliferation ability (Jia et al., 2019; Pacella et al., 2018). The reason why hybrid metabolic phenotype appears in different cells is still unclear. Well, the recent study has suggested that TGF-β may promote glycolysis and upregulate the FAO (fatty acid β-oxidation) to generate the energy simultaneously (Jia et al., 2021). Hence, we gather that, although the enhancement of glycolytic pathway may have an impact on the OXPHOS of the glucose, FAO restored the OXPHOS within limits. Thus, both glycolysis and OXPHOS are relatively active. We believe that this may be the cause of the hybrid metabolic phenotype in fibroblast trans-differentiation. However, the relationship between the metabolic state and the cell fate is very complex, and the reliable mechanism remains to be explored.

Similar with Akt/p38MAPK pathway, we found that the expressions of four epigenetic factors such as Ctcf, Ezh2, Kdm2b, and Wdr5, which were reported to be important pluripotency factors, were significantly upregulated at the initial stage of the induction and then gradually downregulated in the subsequent induction process (Figure 5A). The high expressions of these four factors were considered to be important markers of self-renewal and "stemness" (Ang et al., 2011; Onder et al., 2012; Wang et al., 2011, 2017). In other words, during the process of trans-differentiation, the "stemness" of fibroblasts also increased first

and then decreased. The intermediate state shows the similar characteristics with the early stage of the reprogramming. Recent studies have also shown that the expressions of these four factors are promoted by TGF-β, and this significantly reduces the pluripotency barriers during the reprogramming process (Sun et al., 2020). Since the similar trend with Akt/p38MAPK pathway was observed, we gather that the activation of TGF-β/Akt/p38MAPK axis positively regulated the expression of these four epigenetic factors. However, the specific mechanism of how TGF-β/Akt/p38MAPK axis promotes the expressions of these four epigenetic factors remains unclear and needs further study. At the same time, an important apoptosis gene, Tp53, which is negatively regulated by AKT shows an opposite expression trend to the four factors (Haupt et al., 2003). This result further supports the existence of an intermediate state with "stemness" in the early stage of trans-differentiation.

In order to further show the states of the fibroblasts with different degrees of trans-differentiation under different induction times, we re-cultured each sample in normal medium without TGF-β1. Then, we gave the comparison of the α-Sma expressions before and after the re-culture of each sample (Figure 5B). We can see that the α-Sma expressions of the fibroblasts induced for 1-3 days decreased more than 30% after re-culture. In contrast, the fibroblasts induced for more than 4 days showed very slight changes in α-Sma expressions after 3 days of re-culture. In other words, the fibroblasts in the intermediate state are still on the pathway of trans-differentiation process and will relatively quickly return to the original state if the induction condition is lost. Only when the cells reach and go across the intermediate state, they can maintain the relatively stable state. Then the fibroblast-myofibroblast trans-differentiation process is nearly complete.

Although more and more attentions have been paid to the study of trans-differentiation, it is still unclear whether the intermediate states emerge in the process of trans-differentiation for different cell lineages (Jopling et al., 2011). There are hints for the appearances of the intermediate states in certain other trans-differentiation processes. It has been reported that an intermediate state called XEN-like (extraembryonic endoderm-like) state was identified leading to efficiently reprogramming by chemical induction of mouse fibroblasts (Zhao et al., 2015). Then, these XEN-like cells were directly reprogramed to neurons. This avoids the time-consuming iPSC (induced pluripotent stem cell) generation (Li et al., 2017). During trans-differentiation, fibroblasts may pass through the intermediate state with high pluripotency when the pluripotent features are detected (Treutlein et al., 2016). Furthermore, one can see that the characteristics of the intermediate state of the trans-differentiation in diverse cell lineages are different (Reid and Tursun, 2018). Therefore, our study and findings here enrich the understanding of the possible intermediate states in the trans-differentiation process.

In this study, we show that TGF-β1-induced trans-differentiation from fibroblasts to myofibroblasts is closely related to the Smad and Akt/p38MAPK signaling pathways, without which the trans-differentiation would not be continued. We further induced fibroblasts for 1-7 days. Then, through the analysis of transcriptomic sequencing, changes in cell proliferation capacity, and metabolic reprogramming, we found evidence of an intermediate state in the process of trans-differentiation. In the early stage of trans-differentiation, cells may enter the intermediate state first. And this intermediate state has multiple characteristics such as accelerated cell cycle, OGS, enhanced anti-apoptotic ability, and pluripotency, which is similar to the early stage of reprogramming. As the trans-differentiation continues, these characteristics get switched. The switching of cell proliferation ability, metabolic pathways, and "stemness" promotes the entire progress of trans-differentiation. This supports the possibility of an intermediate state in the trans-differentiation process with cellular characteristic switching. Trans-differentiation appears to be only completed after the cells pass through this intermediate state. Otherwise, the cells are more likely to return to the original state. We expect that the mechanism of this intermediate state is not only in the trans-differentiation from fibroblasts to the fibroblasts but might be common in the process of multiple cell fate switching. Our study has shown the evidence of the possible intermediate state in the process of trans-differentiation and suggests its formation mechanism. This provides a new perspective for a better understanding of the process of cell fate decision-making and switching.

Limitations of the study

Our experiments suggest that there may be a transient hybrid metabolic phenotype in the process of fibroblast-myofibroblast trans-differentiation. We believe that this phenomenon is related to fatty acid metabolism. However, more evidence remains to be seen. In addition, we have not yet fully understood the specific mechanisms of how the TGF-β pathway influences the expressions of several self-renewal epigenetic factors. Lastly, a large amount of data comes from the experimental results of the cell populations. We do not yet know whether the

average effect of the cell populations can accurately reflect the path of the fibroblast-myofibroblast trans-differentiation process at the single-cell level. This requires further exploration.

STAR★METHODS

Detailed methods are provided in the online version of this paper and include the following:

- KEY RESOURCES TABLE
- RESOURCE AVAILABILITY
  - Lead contact
  - Materials availability
  - Data and code availability
- EXPERIMENTAL MODEL AND SUBJECT DETAILS
  - Cell lines
- METHOD DETAILS
  - TGF-β1 induced trans-differentiation
  - RNA extraction and time-course RNA sequencing
  - cDNA synthesis and qPCR
  - Immunofluorescence
  - siRNA transfection and SIS3 inhibitor
  - Seahorse analysis
  - Cell proliferation assay
- QUANTIFICATION AND STATISTICAL ANALYSIS
  - Time-course RNA sequencing data analysis
  - Statistical analysis

SUPPLEMENTAL INFORMATION

Supplemental information can be found online at https://doi.org/10.1016/j.isci.2021.103057.

ACKNOWLEDGMENTS

Z.Y., W.L., Z.J., and E.W. are supported by the National Natural Science Foundation of China, [Grant No, 91430217] & [Grant No, 21721003] and the Ministry of Science and Technology (MOST) of the People's Republic of China [Grant No, 2016YFA0203200].

AUTHOR CONTRIBUTIONS

Z.Y., Z.J., E.W., and J.W. contributed to the experimental design. Z.Y. and Z.J. conducted the experiments. Z.Y., W.L., and Z.J. contributed to data interpretation. Z.Y., Z.J., E.W., and J.W. contributed to writing and revising the manuscript.

DECLARATION OF INTERESTS

The authors declare no competing interests.

Received: March 11, 2021
Revised: July 23, 2021
Accepted: August 25, 2021
Published: September 24, 2021

REFERENCES

Ang, Y.S., Tsai, S.Y., Lee, D.F., Monk, J., Su, J., Ratnakumar, K., Ding, J.J., Ge, Y.C., Darr, H., Chang, B., et al. (2011). Wdr5 mediates self-renewal and reprogramming via the embryonic stem cell core transcriptional network. Cell *145*, 183–197. https://doi.org/10.1016/j.cell.2011.03.003.

Bolanos, J.P. (2013). Adapting glycolysis to cancer cell proliferation: the MAPK pathway focuses on PFKFB3. Biochem. J. *452*. e7–9. https://doi.org/10.1042/bj20130560.

Chang, L.F., and Karin, M. (2001). Mammalian MAP kinase signalling cascades. Nature *410*, 37–40. https://doi.org/10.1038/35065000.

Conte, E., Gili, E., Fagone, E., Fruciano, M., Iemmolo, M., and Vancheri, C. (2014). Effect of pirfenidone on proliferation, TGF-beta-induced myofibroblast differentiation and fibrogenic activity of primary human lung fibroblasts. Eur. J. Pharm. Sci. *58*, 13–19. https://doi.org/10.1016/j.ejps.2014.02.014.

DeBerardinis, R.J., Lum, J.J., Hatzivassiliou, G., and Thompson, C.B. (2008). The biology of cancer: metabolic reprogramming fuels cell growth and proliferation. Cell Metab. *7*, 11–20. https://doi.org/10.1016/j.cmet.2007.10.002.

Ding, H., Jiang, L., Xu, J., Bai, F., Zhou, Y., Yuan, Q., Luo, J., Zen, K., and Yang, J.W. (2017). Inhibiting aerobic glycolysis suppresses renal interstitial fibroblast activation and renal fibrosis.

CellPress
OPEN ACCESS

Am. J. Physiol. Renal Physiol. *313*, F561–F575. https://doi.org/10.1152/ajprenal.00036.2017.

Fritz, V., and Fajas, L. (2010). Metabolism and proliferation share common regulatory pathways in cancer cells. Oncogene *29*, 4369–4377. https://doi.org/10.1038/onc.2010.182.

Granados-Aparici, S., Hardy, K., Franks, S., Sharum, I.B., Waite, S.L., and Fenwick, M.A. (2019). SMAD3 directly regulates cell cycle genes to maintain arrest in granulosa cells of mouse primordial follicles. Sci. Rep. *9* (12), 6513. https://doi.org/10.1038/s41598-019-42878-4.

Haupt, S., Berger, M., Goldberg, Z., and Haupt, Y. (2003). Apoptosis - the p53 network. J. Cell Sci. *116*, 4077–4085. https://doi.org/10.1242/jcs.00739.

Hinz, N., and Jucker, M. (2019). Distinct functions of AKT isoforms in breast cancer: a comprehensive review. Cell Commun. Signal. *17*, 154. https://doi.org/10.1186/s12964-019-0450-3.

Hua, W., Ten Dijke, P., Kostidis, S., Giera, M., and Hornsveld, M. (2020). TGF beta-induced metabolic reprogramming during epithelial-to-mesenchymal transition in cancer. Cell. Mol. Life Sci. *77*, 2103–2123. https://doi.org/10.1007/s00018-019-03398-6.

Jia, D.Y., Lu, M.Y., Jung, K.H., Park, J.H., Yu, L.L., Onuchic, J.N., Kaipparettu, B.A., and Levine, H. (2019). Elucidating cancer metabolic plasticity by coupling gene regulation with metabolic pathways. Proc. Natl. Acad. Sci. U S A *116*, 3909–3918. https://doi.org/10.1073/pnas.1816391116.

Jia, D.Y., Park, J.H., Kaur, H., Jung, K.H., Yang, S., Tripathi, S., Galbraith, M., Deng, Y.Y., Jolly, M.K., Kaipparettu, B.A., et al. (2021). Towards decoding the coupled decision-making of metabolism and epithelial-to-mesenchymal transition in cancer. Br. J. Cancer *124*, 1902–1911. https://doi.org/10.1038/s41416-021-01385-y.

Jolly, M.K., Jia, D., Boareto, M., Mani, S.A., Pienta, K.J., Ben-Jacob, E., and Levine, H. (2015). Coupling the modules of EMT and stemness: a tunable 'stemness window' model. Oncotarget *6*, 25161–25174. https://doi.org/10.18632/oncotarget.4629.

Jones, R.G., Plas, D.R., Kubek, S., Buzzai, M., Mu, J., Xu, Y., Birnbaum, M.J., and Thompson, C.B. (2005). AMP-activated protein kinase induces a p53-dependent metabolic checkpoint. Mol. Cell *18*, 283–293. https://doi.org/10.1016/j.molcel.2005.03.027.

Jopling, C., Boue, S., and Belmonte, J.C.I. (2011). Dedifferentiation, transdifferentiation and reprogramming: three routes to regeneration. Nat. Rev. Mol. Cell Biol. *12*, 79–89. https://doi.org/10.1038/nrm3043.

Lai, L., Reineke, E., Hamilton, D.J., and Cooke, J.P. (2019). Glycolytic switch is required for transdifferentiation to endothelial lineage. Circulation *139*, 119–133. https://doi.org/10.1161/circulationaha.118.035741.

Li, B., and Wang, J.H.C. (2011). Fibroblasts and myofibroblasts in wound healing: force generation and measurement. J. Viab. *20*, 108–120. https://doi.org/10.1016/j.jtv.2009.11.004.

Li, L., Chen, K., Wang, T., Wu, Y., Xing, G., Chen, M., Hao, Z., Zhang, C., Zhang, J., Ma, B., et al. (2020). Glis1 facilitates induction of pluripotency via an epigenome-metabolome-epigenome signalling cascade. Nat. Metab. *2*, 882–892. https://doi.org/10.1038/s42255-020-0267-9.

Li, X., Liu, D.F., Ma, Y.T., Du, X.M., Jing, J.Z., Wang, L.P., Xie, B.Q., Sun, D., Sun, S.Q., Jin, X.Q., et al. (2017). Direct reprogramming of fibroblasts via a chemically induced XEN-like state. Cell Stem Cell *21*, 264. https://doi.org/10.1016/j.stem.2017.05.019.

Liang, C., Shi, S., Qin, Y., Meng, Q.C., Hua, J., Hu, Q.S., Ji, S.R., Zhang, B., Xu, J., and Yu, X.J. (2020). Localisation of PGK1 determines metabolic phenotype to balance metastasis and proliferation in patients with SMAD4-negative pancreatic cancer. Gut *69*, 888–900. https://doi.org/10.1136/gutjnl-2018-317163.

Liu, X., Li, P., Liu, P., Xiong, R.P., Zhang, E., Chen, X.Y., Gu, D.Y., Zhao, Y., Wang, Z.G., and Zhou, Y.G. (2008). The essential role for c-Ski in mediating TGF-beta 1-induced bi-directional effects on skin fibroblast proliferation through a feedback loop. Biochem. J. *409*, 289–297. https://doi.org/10.1042/bj20070545.

Lu, M., Jolly, M.K., Levine, H., Onuchic, J.N., and Ben-Jacob, E. (2013). MicroRNA-based regulation of epithelial-hybridmesenchymal fate determination. Proc. Natl. Acad. Sci. U S A *110*, 18144–18149. https://doi.org/10.1073/pnas.1318192110.

Meng, X.M., Nikolic-Paterson, D.J., and Lan, H.Y. (2016). TGF-beta: the master regulator of fibrosis. Nat. Rev. Nephrol. *12*, 325–338. https://doi.org/10.1038/nrneph.2016.48.

Onder, T.T., Kara, N., Cherry, A., Sinha, A.U., Zhu, N., Bernt, K.M., Cahan, P., Mancarci, B.O., Unternaehrer, J., Gupta, P.B., et al. (2012). Chromatin-modifying enzymes as modulators of reprogramming. Nature *483*, 598–602. https://doi.org/10.1038/nature10953.

Pacella, I., Procaccini, C., Focaccetti, C., Miacci, S., Timperi, E., Faicchia, D., Severa, M., Rizzo, F., Coccia, E.M., Bonacina, F., et al. (2018). Fatty acid metabolism complements glycolysis in the selective regulatory T cell expansion during tumor growth. Proc. Natl. Acad. Sci. U S A *115*, E6546–E6555. https://doi.org/10.1073/pnas.1720113115.

Pardali, K., Kowanetz, M., Heldin, C.H., and Moustakas, A. (2005). Smad pathway-specific transcriptional regulation of the cell cycle inhibitor p21(WAF1/Cip1). J. Cell. Physiol. *204*, 260–272. https://doi.org/10.1002/jcp.20304.

Reid, A., and Tursun, B. (2018). Transdifferentiation: do transition states lie on the path of development? Curr. Opin. Microbiol. *11*, 18–23. https://doi.org/10.1016/j.coisb.2018.07.004.

Roche, P.L., Filomeno, K.L., Bagchi, R.A., and Czubryt, M.P. (2015). Intracellular signaling of cardiac fibroblasts. Compr. Physiol. *5*, 721–760. https://doi.org/10.1002/cphy.c140044.

Rodriguez, P., Sassi, Y., Troncone, L., Benard, L., Ishikawa, K., Gordon, R.E., Lamas, S., Laborda, J., Hajjar, R.J., and Lebeche, D. (2019). Deletion of delta-like 1 homologue accelerates fibroblast-myofibroblast differentiation and induces myocardial fibrosis. Eur. Heart J. *40*, 967–978. https://doi.org/10.1093/eurheartj/ehy188.

Schruf, E., Schroeder, V., Kuttruff, C.A., Weigle, S., Krell, M., Benz, M., Bretschneider, T., Holweg, A., Schuler, M., Frick, M., et al. (2019). Human lung fibroblast-to-myofibroblast transformation is not driven by an LDH5-dependent metabolic shift towards aerobic glycolysis. Respir. Res. *20*, 87. https://doi.org/10.1186/s12931-019-1058-2.

Smith, P.C. (2018). Role of myofibroblasts in normal and pathological periodontal wound healing. Oral Dis. *24*, 26–29. https://doi.org/10.1111/odi.12773.

Sun, H., Yang, X., Liang, L.N., Zhang, M.D., Li, Y., Chen, J.L., Wang, F.H., Yang, T.T., Meng, F., Lai, X.W., et al. (2020). Metabolic switch and epithelial-mesenchymal transition cooperate to regulate pluripotency. Embo J. *39*, e102961. https://doi.org/10.15252/embj.2019102961.

Ten Dijke, P.T., Goumans, M.J., Itoh, F., and Itoh, S. (2002). Regulation of cell proliferation by Smad proteins. J. Cell. Physiol. *191*, 1–16. https://doi.org/10.1002/jcp.10066.

Tomasek, J.J., Gabbiani, G., Hinz, B., Chaponnier, C., and Brown, R.A. (2002). Myofibroblasts and mechano-regulation of connective tissue remodelling. Nat. Rev. Mol. Cell Biol. *3*, 349–363. https://doi.org/10.1038/nrm809.

Treutlein, B., Lee, Q.Y., Camp, J.G., Mall, M., Koh, W., Shariati, S.A.M., Sim, S., Neff, N.F., Skotheim, J.M., Wernig, M., and Quake, S.R. (2016). Dissecting direct reprogramming from fibroblast to neuron using single-cell RNA-seq. Nature *534*, 391. https://doi.org/10.1038/nature18323.

Wang, F., Han, J.H., Wang, L., Jing, Y., Zhu, Z., Hui, D.W., Wang, Z.H., Wang, Y.Z., Dong, Y., and Tan, T. (2017). CCCTC-binding factor transcriptionally targets Wdr5 to mediate somatic cell reprogramming. Stem Cells Dev. *26*, 743–750. https://doi.org/10.1089/scd.2016.0309.

Wang, T., Chen, K.S., Zeng, X.M., Yang, J.G., Wu, Y., Shi, X., Qin, B.M., Zeng, L.W., Esteban, M.A., Pan, G.J., and Pei, D.Q. (2011). The histone demethylases Jhdm1a/1b enhance somatic cell reprogramming in a vitamin-C-dependent manner. Cell Stem Cell *9*, 575–587. https://doi.org/10.1016/j.stem.2011.10.005.

Xie, N., Tan, Z., Banerjee, S., Cui, H.C., Ge, J., Liu, R.M., Bernard, K., Thannickal, V.J., and Liu, G. (2015). Glycolytic reprogramming in myofibroblast differentiation and lung fibrosis. Am. J. Respir. Crit. Care Med. *192*, 1462–1474. https://doi.org/10.1164/rccm.201504-0780OC.

Yang, J., Antin, P., Berx, G., Blanpain, C., Brabletz, T., Bronner, M., Campbell, K., Cano, A., Casanova, J., Christofori, G., et al. (2020). Guidelines and definitions for research on epithelial-mesenchymal transition. Nat. Rev. Mol. Cell Biol. *21*, 341–352. https://doi.org/10.1038/s41580-020-0237-9.

Yeh, H.W., Lee, S.S., Chang, C.Y., Lang, Y.D., and Jou, Y.S. (2019). A new switch for TGF beta in cancer. Cancer Res. *79*, 3797–3805. https://doi.org/10.1158/0008-5472.Can-18-2019.

Zeglinski, M.R., Roche, P., Hnatowich, M., Jassal, D.S., Wigle, J.T., Czubryt, M.P., and Dixon, I.M.C. (2016). TGF beta(1) regulates Scleraxis expression in primary cardiac myofibroblasts by a Smad-independent mechanism. Am. J. Physiol. Heart Circul. Physiol. *310*, H239–H249. https://doi.org/10.1152/ajpheart.00584.2015.

Zhang, W., Ping, J., Zhou, Y., Chen, G., and Xu, L. (2019). Salvianolic acid B inhibits activation of human primary hepatic stellate cells through downregulation of the myocyte enhancer factor 2 signaling pathway. Front. Pharmacol. *10*, 322. https://doi.org/10.3389/fphar.2019.00322.

Zhao, Y., Zhao, T., Guan, J.Y., Zhang, X., Fu, Y., Ye, J.Q., Zhu, J.L., Meng, G.F., Ge, J., Yang, S.S., et al. (2015). A XEN-like state bridges somatic cells to pluripotency during chemical reprogramming. Cell *163*, 1678–1691. https://doi.org/10.1016/j.cell.2015.11.017.

STAR★METHODS

KEY RESOURCES TABLE

REAGENT or RESOURCE	SOURCE	IDENTIFIER
Antibodies		
rabbit monoclonal anti-α-Sma	Abcam	Cat# ab124964, RRID:AB_11129103
rabbit monoclonal anti-Col1a1	Bioss	Cat# bs-20124R, RRID:AB_2892987
rabbit monoclonal anti-Fibronectin	Abcam	Cat# ab45688, RRID:AB_732380
goat polyclonal antibody to rabbit IgG-H&L (Alexa Fluor® 488)	Abcam	Cat# ab150077, RRID:AB_2630356
Chemicals, peptides, and recombinant proteins		
TGF-β1	Peprotech	Cat# 100-21, Lot.No. 1020209
Paraformaldehyde	Biosharp Life Sciences	Cat# BL539A Lot. No.69080900 CAS: 30525-89-4
Triton X-100	Solarbio Life Sciences	Cat# T8200, Lot. No. 1109F0511, CAS:9002-93-1
Tween 20	Solarbio Life Sciences	Cat# T8220 Lot. No.129T0111 CAS:9005-64-5
BSA	Equitech-Bio	Cat# BAH67 Lot. No.BAH67-1272 CAS: 9048-46-8
Glycine	Aladdin Biochemical Technology	Cat# A111465, Lot. No.E2117043, CAS:56-40-6
DAPI	Bioss	Cat# S0001, Lot. No.BA01158186 CAS: 47165-04-8
SIS3 HCl	Selleck	S7959 CAS: 521984-48-5
Critical commercial assays		
UNIQ-10 Column Trizol Total RNA Isolation Kit	Sangon Biotech	REF# B511321-0100, Lot. No. H526KA0176
PrimeScript™ 1st Strand cDNA Synthesis Kit	Takara	Cat# RR047A, Lot. No. AKG0722A
TransStart® Top Green qPCR SuperMix	TransGen Biotech	Cat# AQ131 Lot. No.O10916
riboFECT CP Transfection	Ribobio	Cat# C10511-05, Lot. No. S0827
Seahorse XFp Cell Mito Stress Test Kit (Oligomycin, FCCP and Rotenone AA)	Seahorse	Cat#103010-100 Lot. No.17103106B
Seahorse XFp Glycolysis Stress Test Kit (Glucose, Oligomycin, and 2-DG)	Seahorse	Cat#103017-100 Lot. No.17130216
Deposited data		
Human reference genome NCBI_GCF_000001405.38_GRCh38.p12	Genome Reference Consortium	https://www.ncbi.nlm.nih.gov/assembly/GCF_000001405.38

(*Continued on next page*)

Continued

REAGENT or RESOURCE	SOURCE	IDENTIFIER
Experimental models: Cell lines		
Human dermal fibroblasts (HDFs)	ScienCell Research Laboratories	Cat# 2320, Lot. No.12925
Oligonucleotides		
siRNA targeting sequence of Smad4 CCATCTGAGTCTAATGCTA	Ribobio	Lot. No.S1227
siRNA targeting sequence of Map2k6 GGACTCTGTTGCTAAAACA	Ribobio	Lot. No.S0910
All of the Primers, see Table S1	This Paper	N/A
Software and algorithms		
Graphpad Prism	Prism version 7	www.graphpad.com/scientific-software/prism/ RRID: SCR_002798
Matlab	R2018b	ww2.mathworks.cn RRID:SCR_001622
Other		
Fibroblast Medium	ScienCell Research Laboratories	Cat#2301, Lot. No.27416
T25 flasks	Nest	Cat#707003
Dulbecco's Modifed Eagle Medium (DMEM)	Hyclone	Cat# SH30022.01, Lot. No.AE24921270
Fetal bovine serum	Biological Industries	REF#04-002-1A Lot. No.1903218
6-well plates	Nest	Cat# 703001, Lot. No. 052721BA01

RESOURCE AVAILABILITY

Lead contact

Further information and requests for resources should be directed to and will be fulfilled by the lead contact, Jin Wang (jin.wang.1@stonybrook.edu).

Materials availability

This study did not generate new unique reagents.

Data and code availability

The data of time-course RNA Sequencing was showed in Data S1.

EXPERIMENTAL MODEL AND SUBJECT DETAILS

Cell lines

Human dermal fibroblasts (HDFs) were purchased from ScienCell Research Laboratories and were isolated from adult human skin. The sex of cells was not given by ScienCell Research Laboratories. HDFs were characterized by their spindle morphology and immunofluorescence with antibody specific to fibronectin. HDFs were negative for HIV-1, HBV, HCV, mycoplasma, bacteria, yeast, and fungi. The above cell authentication was verified by ScienCell Research Laboratories. According to the instructions, HDFs were cultured in Fibroblast Medium (ScienCell Research Laboratories) in T25 flasks. Change the medium every other day. When the culture was approximately 90% confluent, cells were passaged into T25 flasks (12.5×10^4 cells). In this study, HDFs were passaged no more than 7 times and cultured in the incubator (Thermo Fisher Scientific) at 37°C and 5% CO_2 supplemented.

METHOD DETAILS

TGF-β1 induced trans-differentiation

When the cells was approximately 90% confluent, HDFs were seeded into 6-well plates (5×10^4 cells/ well). After 24 h, HDFs were firstly pretreated with serum-free DMEM (Dulbecco's Modifed Eagle Medium) overnight to starve the cells on day0. Then the medium was replaced with the low fetal bovine serum (Biological Industries) (0.5%) DMEM containing TGF-β1 (Transforming growth factor β-1) (5 ng/ mL) to induce cells on day1. The medium was changed every day from day1 to day7. For whether the cells will go back to fibroblasts while removing TGF-β1, when the process of the cells induced by TGF-β1 is completed, parts of the cells were taken from each 7 samples and RNAs were extracted. Then, we cultured the remaining cells normally and the TGF-β1 was removed by updating the medium. After three days of non-induced culture, these cells were collected and the RNAs were extracted.

RNA extraction and time-course RNA sequencing

Total RNA was extracted with UNIQ-10 Column Trizol Total RNA Isolation Kit (Sangon Biotech) according to the instructions. Briefly, cells were lysed by Trizol, and then total RNA was collected in the column by centrifuge. After washed by PRE Solution, RNA was collected in DEPC-treated water. A total number of 24 RNA samples were collected at fixed time point from day0 to day7 and 3 independently repeated samples for each day, and then sequenced by DNBSEQ (BGI Tech).

cDNA synthesis and qPCR

cDNA synthesis was performed by using PrimeScript™ 1st Strand cDNA Synthesis Kit (Takara). In brief, 1 μg of RNA was mixed with gDNA Eraser at 42°C for 2 min to deplete genome DNA. Then, RT Enzyme Mix, dNTP Mixture and RT Primer Mix were simultaneously added into the above mixture at 37°C and incubation for 15 min. The final obtained cDNA was stored at -20°C.

The gene expression was detected by real-time PCR (qPCR) with TransStart® Top Green qPCR SuperMix (TransGen). A final 20 μL reaction contains 1 uL of cDNA solution, 10 μL of SYBR Green SuperMix, 6.8 μL water, 0.2 μM forward and reverse primer (Comate Bioscience) (Table S1). After centrifuge, the mixture was loaded in the chip and processed in StepOnePlus™ Real-Time PCR System (Applied Biosystems) following the procedure: 94°C for 30 s followed by 40 cycles of 94°C for 5 s and subsequently 60°C for 30 s.

Immunofluorescence

Cells were washed with PBS (phosphate buffered saline) (Solarbio Life Sciences) 3 times and fixed by 4% paraformaldehyde (Biosharp Life Sciences) for 15 min at room temperature. Then, for α-Sma, the cells were permeated in PBS with 0.1% Triton X-100 (Solarbio Life Sciences). But this step was inapplicable to Fibronectin and Col1a1. After washing 3 times with PBST (PBS with 0.1% Tween 20 (Solarbio Life Sciences)), the cells were immersed in the blocking solution (1% BSA (bovine serum albumin) (Equitech-Bio)) and 22.52 mg/ mL glycine (Aladdin Biochemical Technology) in PBST) for 30 min to block unspecific binding of the antibodies. After that, the above disposed cells were washed by PBST 3 times and incubated with primary antibodies diluted with antibody dilution buffer (1% BSA in PBST) overnight at 4°C. Secondary antibodies were added at room temperature in dark after cells were washed with PBST 3 times. After 45 min, cells were washed with PBS and incubated with DAPI (4',6-Diamidino-2'-phenylindole) staining solution (10 ng/ mL) for 10 min. Further, images were captured by EVOS™ XL Core Imaging System (Thermo Fisher Scientific). All the antibodies for immunofluorescence were listed as follow. Primary antibody of rabbit monoclonal anti-Col1a1 (bs-20124R) (1:500 dilution) was purchased from Bioss Antibodies. Primary antibody of rabbit monoclonal anti-α-Sma (ab124964) (1:300 dilution), rabbit monoclonal anti-Fibronectin (ab45688) (1:1000 dilution) and secondary antibody of goat polyclonal antibody to rabbit IgG-H&L (Alexa Fluor® 488) (ab150077) (1:1000 dilution) were all purchased from Abcam.

siRNA transfection and SIS3 inhibitor

Small interfering RNA (siRNA) was used widely to attenuate gene expression. 10 μg siRNA targeting Smad4 or Map2k6 (Ribobio) was mixed with riboFECT CP Transfection (Ribobio) for 15 min. Then the complex was transfected into HDFs before starvation (day-1). After 24 h, siRNA was removed together with the medium by replaced with serum-free DMEM. The siRNA target sequence of Smad4 and Map2k6 were CCATCT GAGTCTAATGCTA and GGACTCTGTTGCTAAAACA, respectively. Furthermore, to clarify whether the

knockdown of Smad4 or Map2k6 just delays the trans-differentiation or abrogates the trans-differentiation, the siRNA was added into HDFs at day-1, day2 and day5 during the trans-differentiation process.

For testing the SIS3 and TGF-β1 on the expressions of Hk1, Hk2, Hif-1A, Ldha and Glut1, SIS3 (1 μM, dissolved in DMSO, Selleck) and TGF-β1 (5 ng/ mL) were added into HDFs before starvation to inhibit TGF-β/Smad signaling pathway. After 72 h, the RNA was extracted and the expressions were determined by qPCR.

Seahorse analysis

For the HDFs before treating with TGF-β1 (day0) and after treating with TGF-β1 from day1 to day7, cells were collected from each day and then seeded into the XF cell culture plate (6×10^3 cells/ well) (Seahorse XFp) with low serum DMEM. Before seeding, the cells were placed at room temperature for 30 min and then cultured in the incubator overnight. Cells were washed with XF assay media (Seahorse XF) twice before placed in the atmosphere without CO_2. For measurement of OCR (oxygen consumption rate), oligomycin, FCCP and rotenone AA were pre-added into XF sensor cartridge (Seahorse XFp), they were sequentially injected into cell culture plate. For measurement of ECAR (extracellular acidification rate), cells were sequentially treated with glucose, oligomycin, and 2-DG. To reveal the effects of TGF-β1 and SIS3 on glycolysis ability, HDFs were seeded into the XF cell culture plate (6×10^3 cells/ well). After 24 hstarvation, cells were induced by TGF-β1 (5 ng/ mL), SIS3 (1 μM) and both of them, respectively. All of the concentration of compounds was suggested by manufacturer's instructions.

Cell proliferation assay

Cell proliferation was tested by Real Time Cellular Analysis (RTCA) system (xCElligence). Firstly, 50 μL DMEM were added in E-Plate (xCElligence) to balance baseline. Then HDFs (5×10^3 cells/ well) during trans-differentiation of day0 to day7 were seeded at the E-Plate and cell index was observed every 15 min until 30 h. For testing the cell proliferation influenced by TGF-β1 and SIS3, HDFs (5×10^3 cells/ well) were seeded into the E-Plate. After 6 hours, cells were starved with DMEM without serum. 12 hours later, TGF-β1 (5 ng/ mL), SIS3 (1 μM) or both of them were added to induced cells and DMSO was added as the negative control. Cell index was observed every 15 min until 30 h.

QUANTIFICATION AND STATISTICAL ANALYSIS

Time-course RNA sequencing data analysis

After that we got the value of transcription expression and calculated the Spearman's rank correlation coefficient between expression of each gene and time point. These genes with high Spearman rank correlation mainly grouped in the Akt, MAPK, CDK and TGF-β pathways. Then these genes in these pathways were selected for further cluster analysis and clustered through the function cluster gram in matlab 2018. In this process, we used Euclidean distance to generate the hierarchical cluster tree for genes.

Specifically, the RNA Sequencing expression data include 3 samples for each day. First, the RNA Sequencing expression data in one day were averaged and considered as one sample. Then we transformed the standardized values by the function so that the mean was 0 and the standard deviation was 1 in the specified dimension. Finally, hierarchical clustering analysis was performed on the standardized expression data in the gene dimension. And the heatmap of RNA Sequencing expression data from day1 to day7 was acquired.

Statistical analysis

Data are presented as means ± the SD. All data are from at least three independent experiments. The t tests of two groups was analyzed by GraphPad Prism. Differences with p values of less than 0.05 were considered statistically significant.